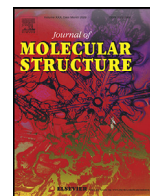




Since January 2020 Elsevier has created a COVID-19 resource centre with free information in English and Mandarin on the novel coronavirus COVID-19. The COVID-19 resource centre is hosted on Elsevier Connect, the company's public news and information website.

Elsevier hereby grants permission to make all its COVID-19-related research that is available on the COVID-19 resource centre - including this research content - immediately available in PubMed Central and other publicly funded repositories, such as the WHO COVID database with rights for unrestricted research re-use and analyses in any form or by any means with acknowledgement of the original source. These permissions are granted for free by Elsevier for as long as the COVID-19 resource centre remains active.



# Molecular insights of hyaluronic acid-hydroxychloroquine conjugate as a promising drug in targeting SARS-CoV-2 viral proteins



R. Thirumalaisamy<sup>a,b</sup>, V. Aroulmoji<sup>c,\*</sup>, Muhammad Nasir Iqbal<sup>d</sup>, M. Deepa<sup>e</sup>, C. Sivasankar<sup>f</sup>, Riaz Khan<sup>g</sup>, T. Selvankumar<sup>a</sup>

<sup>a</sup> Department of Biotechnology, Mahendra Arts & Science College (Autonomous), Namakkal (Dt.) - 637 501, Tamil Nadu, India

<sup>b</sup> Department of Biotechnology, Sona College of Arts and Science, Salem (Dt.) -636 005, Tamil Nadu, India

<sup>c</sup> Centre for Research & Development, Mahendra Engineering College (Autonomous), Mallasamudram, Namakkal (Dt.) - 637 503, Tamil Nadu, India

<sup>d</sup> Department of Biosciences, COMSATS University, Islamabad Campus, Islamabad, Pakistan

<sup>e</sup> Postgraduate and Research Department of Chemistry, Muthurangam Govt. Arts College, Vellore, India

<sup>f</sup> Catalysis and Energy Laboratory, Department of Chemistry, Pondicherry University, R.V.Nagar, Kalapet, Pondicherry, 605014, India

<sup>g</sup> Rumsey, Old Bath Road, Sonning, Berkshire, RG4 6TA, England, United Kingdom

## ARTICLE INFO

### Article history:

Received 21 December 2020

Revised 5 April 2021

Accepted 7 April 2021

Available online 13 April 2021

### Keywords:

HA-HCQ

HCQ

SARS-CoV-2

Main protease

Spike protein

CD44

COVID-19

Docking studies

Hyaluronic acid

## ABSTRACT

*In-silico* anti-viral activity of Hydroxychloroquine (HCQ) and its Hyaluronic Acid-derivative (HA-HCQ) towards different SARS-CoV-2 protein molecular targets were studied. Four different SARS-CoV-2 proteins molecular target i.e., three different main proteases and one helicase were chosen for *In-silico* anti-viral analysis. The HA-HCQ conjugates exhibited superior binding affinity and interactions with all the screened SAR-CoV-2 molecular target proteins with the exception of a few targets. The study also revealed that the HA-HCQ conjugate has multiple advantages of efficient drug delivery to its CD44 variant isoform receptors of the lower respiratory tract, highest interactive binding affinity with SARS-CoV-2 protein target. Moreover, the HA-HCQ drug conjugate possesses added advantages of good biodegradability, biocompatibility, non-toxicity and non-immunogenicity. The prominent binding ability of HA-HCQ conjugate towards Mpro (PDB ID 5R82) and Helicase (PDB ID 6ZSL) target protein as compared with HCQ alone was proven through MD simulation analysis. In conclusion, our study suggested that further *in-vitro* and *in-vivo* examination of HA-HCQ drug conjugate will be useful to establish a promising early stage antiviral drug for the novel treatment of COVID-19.

© 2021 Elsevier B.V. All rights reserved.

## 1. Introduction

The treatment of COVID-19 viral disease, remains challenging; it is a global issue, which requires both the national and the global approaches. To save lives an efficient and safe prescription drug for the disease is urgently needed. Several antiviral drugs have been considered for the treatment of the disease such as Hydroxychloroquine (HCQ), Lopinavir, Ritonavir, Favipiravi, and Remdesivir; the later originally used for the Ebola virus disease, MERS and SARS viruses have been recommended for COVID-19. Although the above-mentioned drugs show positive activity towards the disease, almost all of these drugs are associated with few disadvantages such as insolubility, some toxicity, instability, and kidney clearance [1,2].

Based on our research work on pharmacologically important drugs such as camptothecin, methotrexate, methylprednisolone, propofol to improve their efficacy and targeting delivery for the treatment of diseases such as cancer, arthritis, osteoporosis and anaesthetics respectively; we have developed a unique technology, according to which, the drugs were specifically and covalently linked to the hyaluronic acid (HA) molecule, a natural biopolymer, biocompatible, ubiquitously present in the human and animal body, to afford new drugs, new chemical entities, possessing the unique biological functionalities and properties of both the components synergistically; the evidence is available that the conjugation of drugs with macromolecules enhances the pharmacokinetic profiles of the drugs themselves [3–5].

Hyaluronic acid (HA) generally referred to as Hyaluronan is an anionic, non-sulfated mucopolysaccharide spreading widely throughout the connective and epithelial tissues of animals. HA is one of the main components of the extracellular matrix (ECM) and contributes significantly to the activation of signaling path-

\* Corresponding author.

E-mail address: [aroulmoji@mahendra.info](mailto:aroulmoji@mahendra.info) (V. Aroulmoji).

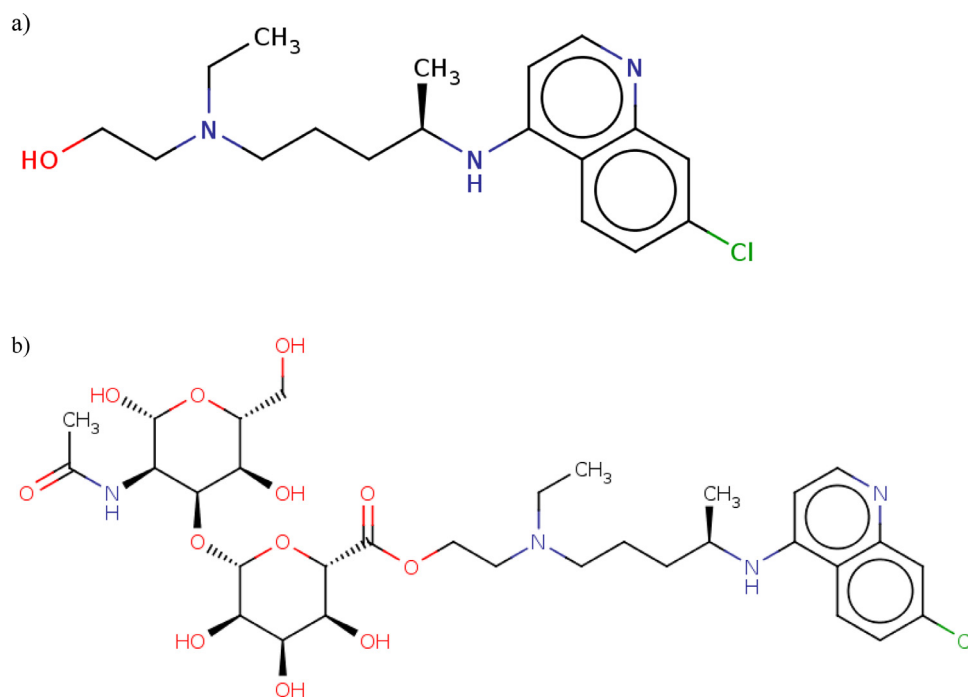


**Fig. 1.** a & b - Structure of Hydroxychloroquine (HCQ) and Hyaluronic acid - Hydroxychloroquine Conjugate (HA-HCQ).

ways that regulate cell proliferation, differentiation, adhesion, and migration [6–9]. It mediates its biological functions through various protein receptors present on different cell surfaces including CD44 [10], HARE [11], RHAMM [12], and LYVE [13].

HA is suitable for various chemical modifications easily in the position of hydroxyl, carboxyl, and N-acetyl functional groups; for example, HA-drug conjugates are used as drug carriers to sustained release, transdermal absorption, and to improve drug targeting [14]. In order to exploit its unique biological properties we have developed a technology, according to which, the drugs were specifically and covalently linked to the hyaluronic acid (HA) molecule of a specific molecular weight and at a specific position to afford a new drug contributing synergistically the pharmacological properties of both the components. We have employed this principle to produce a number of pharmacologically important drugs such as HA-Camptothecin, HA-Methotrexate, HA-Methylprednisolone, and HA-Propofol with improved efficacy and targeted delivery for the treatment of diseases such as cancer, arthritis, osteoporosis and anaesthetics respectively [14,15].

Hydroxychloroquine (HCQ) is a conventional anti-malarial drug with efficiency in several clinical disease conditions like Q fever, rheumatoid arthritis, lupus, sarcoidosis and so on. The mechanism of action by hydroxychloroquine is that of increasing the lysosomal pH of antigen-presenting cells thereby inhibiting the autophagy process. The SARS CoV-2 anti-viral effects of HCQ have also been linked to a mechanism involving interference of SARS-CoV-2 cellular receptor ACE-2 (angiotensin-converting enzyme-2) glycosylation [16]. The observed major side-effects are diarrhea, headache and muscle fatigue. The HCQ produces supplemented early virological immune response against hepatitis C and also reduces HIV-1 cell count [17,18]. Importantly, it has immune-suppressive properties which may be helpful to reduce the risk associated with severe COVID cytokine storm [19].

Our objective is to propose a novel and efficient drug for COVID-19 disease, using an old and well-known antiviral drug, Hydroxychloroquine (HCQ), covalently linking it at a specific position with the Hyaluronic acid (HA) to afford HA-HCQ conjugate to increase its bioavailability, safe, improve its localization, con-

trolled release in the body, enhance its overall efficiency, and eliminate or reduce HCQ's systemic toxicity [14,20,21]. The conjugation of HCQ to hyaluronic acid can be accomplished through the HCQ hydroxyl group to the hyaluronic acid C5' carboxylic group of the glucuronic moiety via an ester linkage. In this scenario, the proposed HA-HCQ conjugate and HCQ are tested separately through molecular docking studies for against four different SARS-CoV-2 target proteins, an efficient drug target for the treatment of COVID-19.

## 2. Methods

### 2.1. Ligand generation

The 2D structure of Hydroxychloroquine (HCQ) and Hyaluronic Acid-Hydroxychloroquine Conjugate (HA-HCQ) are drawn in ACD-Chemsketch and saved as mol format file (Fig. 1 a & b) [22]. The retrieved 2D SDF file format of HCQ and HA-HCQ conjugate structure was submitted to "Online SMILES convertor and Structure file generator", and converted into 3D PDB format [23].

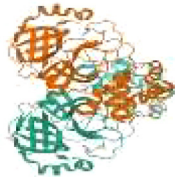
### 2.2. Prediction of drug metabolism and bioavailability profile

PreADMET online server was used to calculate bioavailability and the metabolic score of drug HCQ and its conjugate form

**Table 1**  
Prediction of drug metabolism and bioavailability profile of HCQ and HA-HCQ conjugate.

S.No	PHARMACOKINETIC PROPERTIES	Drug Molecule	
		HCQ	HA-HCQ Conjugate
1.	BIOAVAILABILITY		
	Buffer Solubility (mg/l)	12.91	22.04
	Pure Water Solubility (mg/l)	224.78	261.32
2.	METABOLISM		
	CYP_1A2 Inhibitor	Yes	No
	CYP_2C19_inhibitor	No	No
	CYP_2C9_inhibitor	No	No
	CYP_2D6_inhibitor	Yes	No
	CYP_3A4_inhibitor	Yes	No

**Table 2**  
COVID-19 proteins targets and its 3D docking Score with HCQ and HA-HCQ conjugate.

S.No.	COVID-19 Protein Targets PDB Code	Target Protein Details	Protein 3D Structure	Docking Score (KJ/mol)	
				HCQ	HA-HCQ
1.	5R80	Crystal Structure of COVID-19 main protease in complex with Z18197050		-11.2786	-19.2875
2.	5R82	Crystal Structure of COVID-19 main protease in complex with Z219104216		-12.7873	-22.4332
3.	6Y84	SARS-CoV-2 main protease with unliganded active site (2019-nCoV, coronavirus disease 2019, COVID-19)		-12.2217	-13.2046
4.	6ZSL	Crystal structure of the SARS-CoV-2 Helicase		-13.6327	-23.1778

**Table 3**  
Molecular interaction of HCQ and HA-HCQ conjugate with different COVID-19 protein targets.

S.No.	COVID-19 Proteins Target PDB ID	Ligands	Docking Score (KJ/mol)	No. of Non Bonded Interactions	No. of Hydrogen Bonds	Residue of SARS-CoV-2 Target Proteins involved in Hydrogen bonded Interactions with Ligands
1.	5R80	HCQ	-11.2786	6	4	Ile152*, Tyr154, Val303*, Thr304*
		HA-HCQ	-19.2875	7	7	Leu141*, Asn142*, Gly143*, Ser144, Cys145*, His163, Glu166*
2.	5R82	HCQ	-12.7873	7	4	Ile152*, Tyr154*, Val303*, Thr304*
		HA-HCQ	-22.4332	9	5	Leu141*, Asn142*, His164, Glu166, Gln189
3.	6Y84	HCQ	-12.2217	4	2	Asp153*, Thr304*
		HA-HCQ	-13.2046	10	6	Phe3, Arg4, Trp207, Leu282, Glu288, Asp289
4.	6ZSL	HCQ	-13.6327	11	3	Lys192*, Thr214*, Arg339
		HA-HCQ	-23.1778	9	6	Asp160*, Tyr211*, Gly213*, Thr216*, Tyr217*, Glu341*

**Legend** - \* symbol denotes residues with both Hydrogen and Non bonded Interactions.

(HA-HCQ) to proven “Hyaluronan Drug Delivery (HDD)” technology. Since hyaluronic acid is one of the main components of extracellular matrix (ECM) serving as the ligand of receptor glycoprotein CD44 (cluster of differentiation 44) and RHAMM (receptor for hyaluronan mediated motility), we used hyaluronic acid as a targeting drug carrier for new drug development, HCQ and its conjugate form (HA-HCQ) to show that the drug-carrier conjugate form (HA-HCQ) is less harmful, it is more stable and bio-available as it can be tested for pharmacokinetic properties. It is important to mention here that the drug and its conjugate form, having many differences in molecular weight and its complex structure, produce somewhat different results on computational drug profile results and therefore this study is designed to screen these two parameters and omitting other drug profiles.

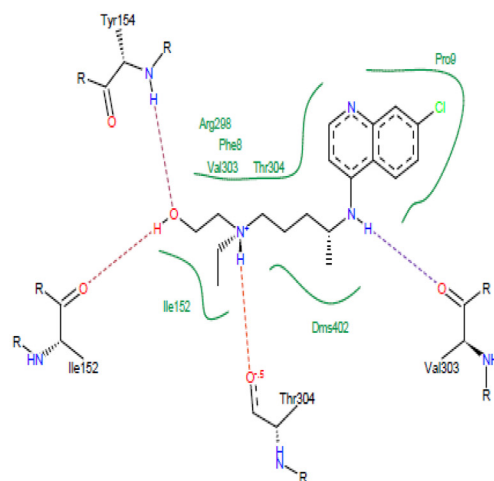
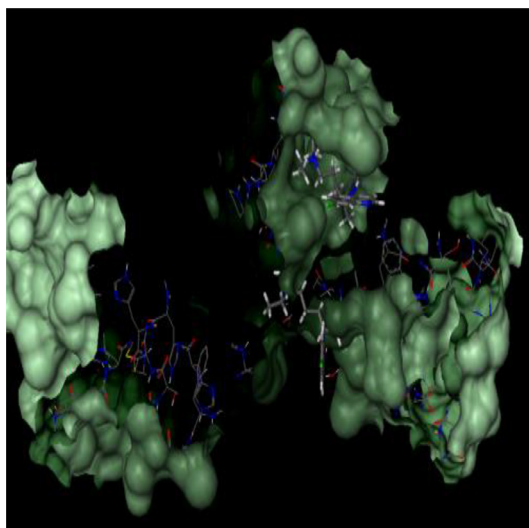
### 2.3. Preparation of receptor and its binding site

Two different types (Mpro and Helicase) of molecular target proteins from novel coronavirus (SARS COV-2 or nCoV-

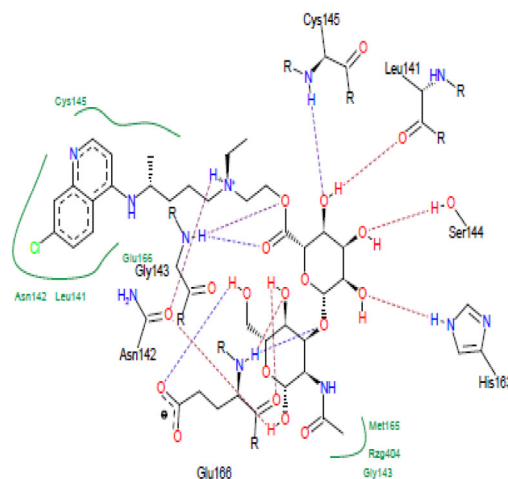
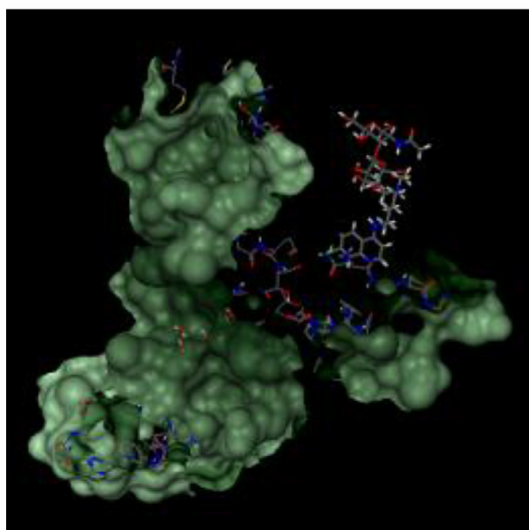
2019) are the key viral molecules involved in the attachment, replication and reproduction of viral particles in the human host cells. These protein molecules served as targets to inhibit the viral lifecycle in human host cells. Four three dimensional crystal structures of SARS-CoV-2, of which three molecules of main protease complex with different inhibitors (5R80, 5R82, 6Y84) and one Helicase protein (6ZSL) were retrieved from the RCSB PDB database and used for the docking studies (<https://www.rcsb.org/>) [24]. To determine the binding affinities between the ligand and COVID-19 receptors, the amino acids with the binding pockets were predicted at the Q-site finder server [25].

### 2.4. Flexible docking

The generated HCQ and HA-HCQ conjugate SDF structures were docked with the predicted binding site of all selected protein target binding site by using FlexX docking software with the



**a) Docking Pose and Interaction plot for 5R80 HCQ Complex (Binding Energy- 11.2786KJ/mol)**



**b) Docking Pose and Interaction plot for 5R80-HA-HCQ Complex (Binding Energy - 25.7233KJ/mol)**

**Fig. 2.** a & b - Docking Pose and Interaction for SARS-CoV-2 main protease 5R80 with HCQ and HA-HCQ conjugate.

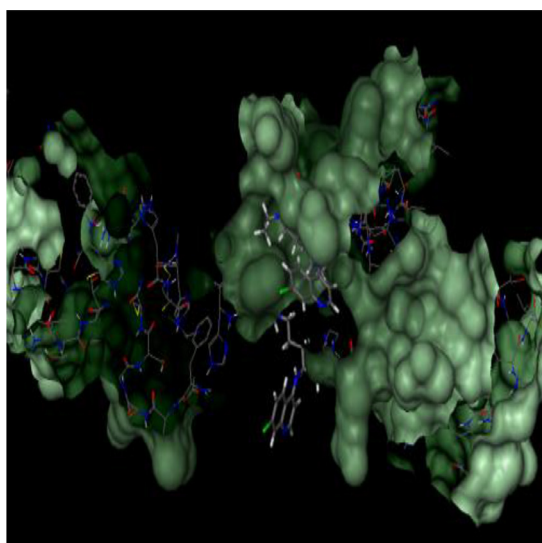
following parameters: (i) default general docking information's (ii) base placement using triangle matching, (iii) scoring of full score contribution and threshold of 0.70, (iv) chemical parameters of clash handling values for protein-ligand clashes with maximum allowed overlap volume of 2.9 Å<sup>3</sup> and intra-ligand clashes with clash factor of 0.6 considering the hydrogen in internal clash tests, and (v) Default docking detail values of 200 for both the maximum number of solutions per iteration and the maximum number of solutions per fragmentation.

### 2.5. Prediction of ligand-receptor interactions

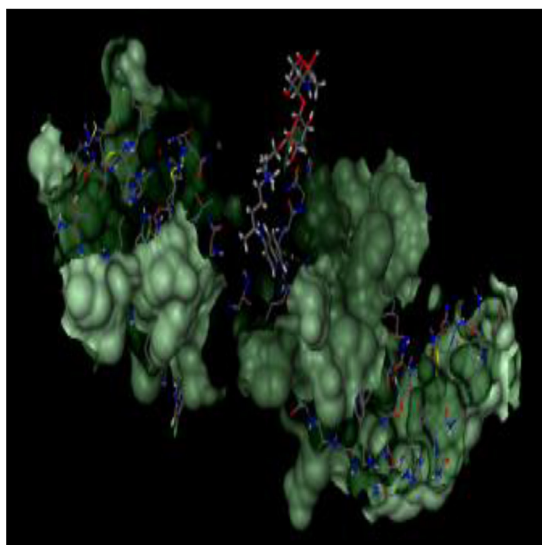
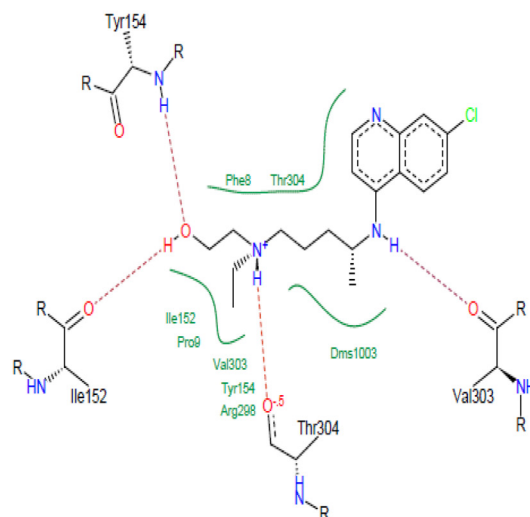
The interactions of HCQ and HA-HCQ with sixteen SARS COV-2 protein targets in the docked complexes were analyzed by the pose-view of LeadIT [25]. The 2D and 3D pose views of SARS COV-2 target protein-ligand complexes were generated and analyzed using LeadIT.

### 2.6. Molecular dynamics simulations

The Molecular Dynamic (MD) Simulations method was employed to predict the ligand binding status of HCQ and HA-HCQ in ligand-protein complexes of HCQ-Mpro (PDB ID 5R82), HAHCQ-Mpro (PDB ID 5R82), HCQ-Helicase (PDB ID 6ZSL) and HAHCQ-Helicase (PDB ID 6ZSL). The MD simulations were run using the Desmond Simulation Package of Schrodinger Suite [26]. The best ligand conformers obtained from molecular docking studies were subjected to molecular dynamics simulations. Protein-ligand complexes were prepared for simulations by using the default parameters of Schrodinger Maestro through the Protein Preparation Wizard tool [27]. Transferable Intermolecular Interaction Potential 3 Points was selected as the solvent model with an orthorhombic box of 10 × 10 × 10 Å. The system was made electrically neutral by adding appropriate counter ions. OPLS\_2005 force field parameters [28] were utilized for the simulations study. The model systems



a) Docking Pose and Interaction plot for 5R82-HCQ Complex (Binding Energy-15.0460KJ/mol)



b) Docking Pose and Interaction plot for 5R82-HA-HCQ Complex (Binding Energy-13.4732KJ/mol)

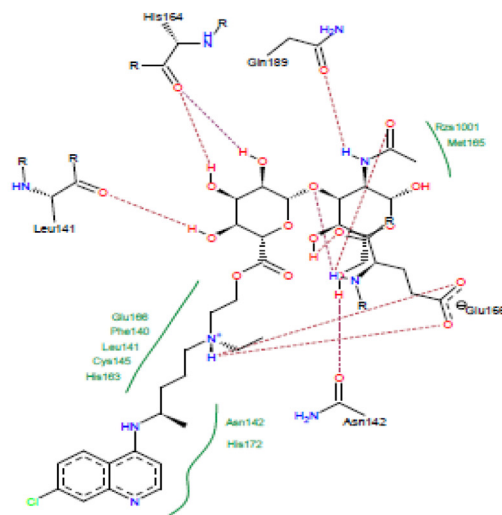


Fig. 3. a & 3b - Docking Pose and Interaction for SARS-CoV-2 spike glycoprotein 6VSB with HCQ and HA-HCQ conjugate.

were relaxed before the simulations. At 300 K temperature and 1 atm pressure with NPT ensemble was applied for all MD simulations. Also, salt at the concentration of 0.15 M was added to mimic physiological conditions. The complexes were subjected to molecular dynamics simulation for 1–50 ns. The Cut-off radius for the Coulombic interactions was set at 9 Å. Nos\_e-Hoover chain thermostat (with a relaxation time of 1 ps) used for controlling the temperature and the Martyna-Tobias-Klein chain barostat (with a relaxation time of 2 ps) were used for pressure. The RESPA integrator utilized for calculating non-bonded forces. The trajectories of MD simulation saved at every 50 ps intervals and the simulations stabilities were evaluated using RMSD of the proteins and ligands over time. The MD simulations were repeated thrice for each complex using the same parameters. All MD simulations studies were carried out using Dell Precision T5810 Workstation with an Nvidia GeForce GTX 1070 8GB graphics processing unit (GPU).

### 3. Results and discussion

#### 3.1. Prediction of drug metabolism and bioavailability profile

The prediction of the drug and its conjugate form metabolism and bioavailability profile were screened through preADMET web server and the results are presented in Table 1. It is quite interesting that the bioavailability parameters such as buffer and pure water solubility of HA-HCQ conjugate are found to be 22.04 mg/l and 261.32 mg/l respectively, which are more than its HCQ drug bioavailability scores of 12.91 mg/l and 224.78 mg/l respectively. It is also interesting to mention here that the metabolic profile of HA-HCQ shows no inhibition against all screened cytochrome drug-metabolizing xenobiotic enzymes such as CYP\_1A2, CYP\_2C19, CYP\_2C9, CYP\_2D6, CYP\_3A4 whereas HCQ shows its inhibitory action against three out of five screened mitochondrial

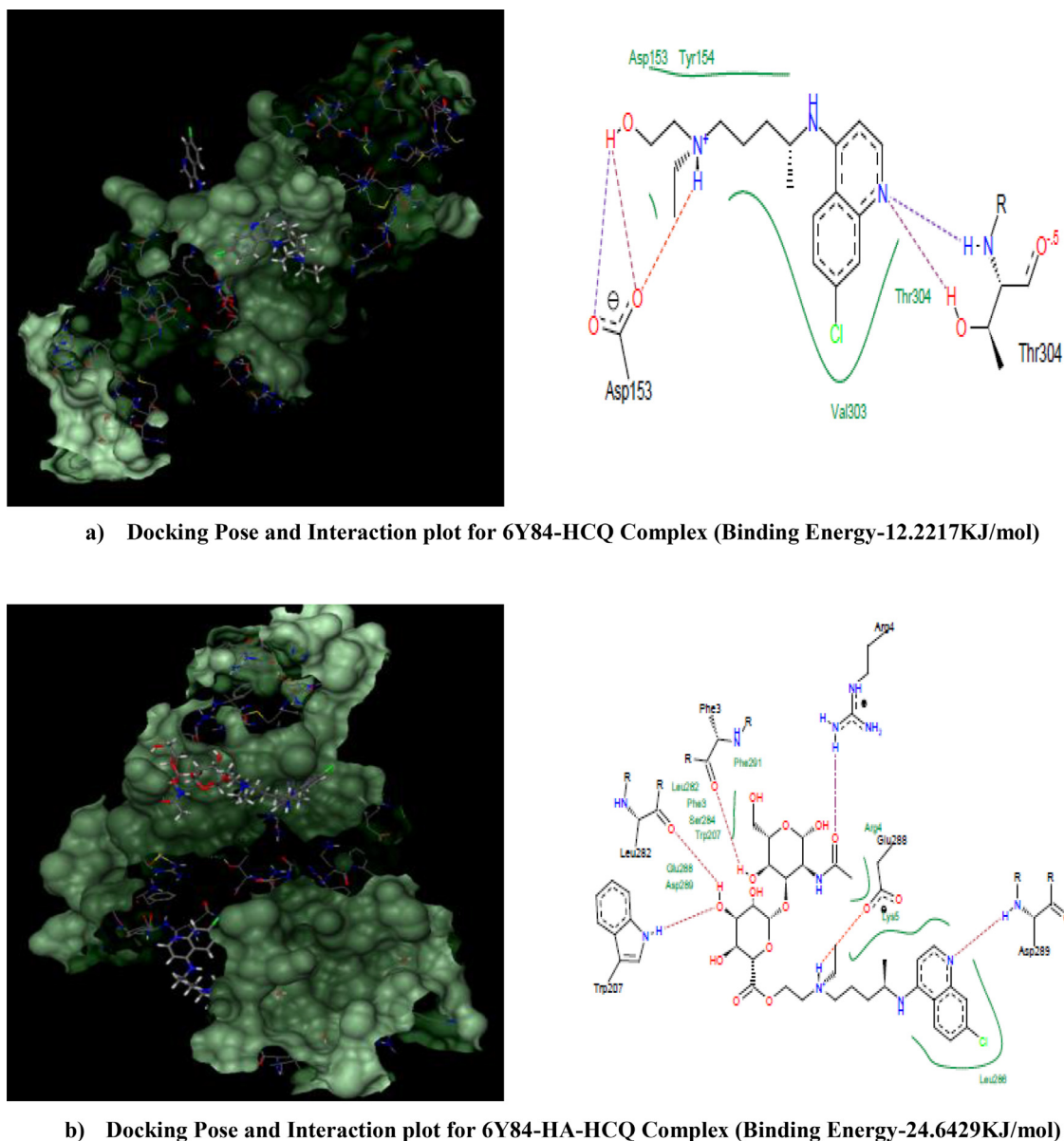


**Fig. 4.** a & 4 b - Docking Pose and Interaction for SARS-CoV-2 main protease 6Y84 with HCQ and HA-HCQ conjugate.

enzymes such as CYP\_1A2, CYP\_2D6, CYP\_3A4. The above results revealed that HA-HCQ conjugate shown more bioavailability, less toxicity and ease of clearance from the body when compared to its free form of drug HCQ. It is worth mentioning here that conjugation of drug with hyaluronic acid enhances the pharmacokinetic profiles of the drugs themselves.

### 3.2. Docking study

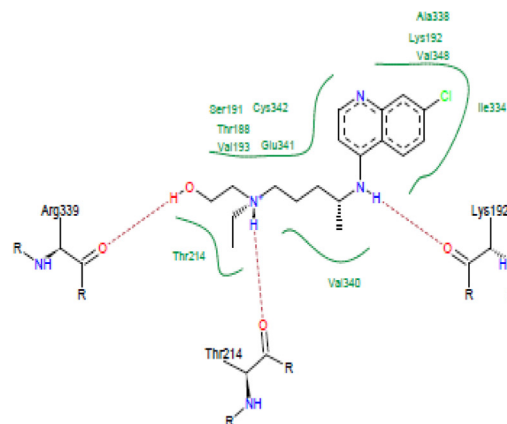
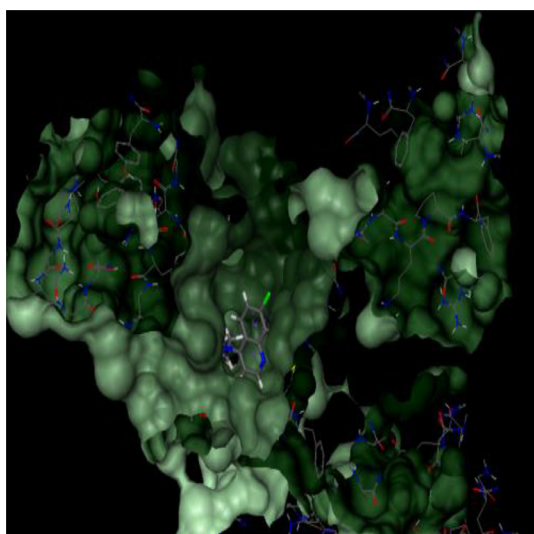
Four different COVID-19 target proteins including three main proteases, one helicase, their docking score and 3D crystal structure are reported in Table 2, and their detailed molecular interaction between the viral target protein and its ligands (HCQ and HA-HCQ conjugate) are tabulated and presented in Table 3 & Figs. 2–5.

The results of flexible docking study using FlexX software between COVID-19 viral targets and HA-HCQ showed the binding affinity and docking score ranging from -13.2046 KJ/mol to -23.1778 KJ/mol whereas HCQ against COVID-19 viral targets shown binding affinity and docking score ranging from -12.2217 KJ/mol to

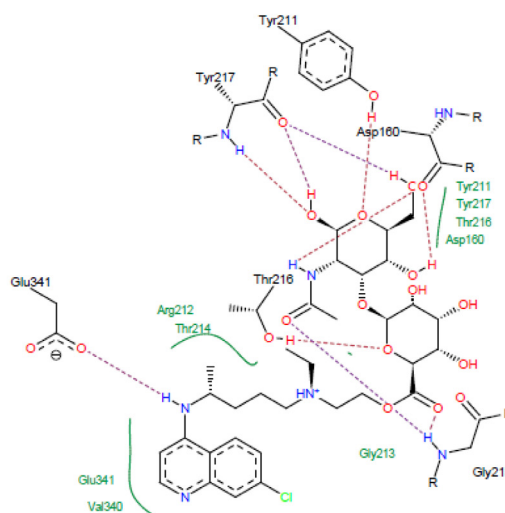
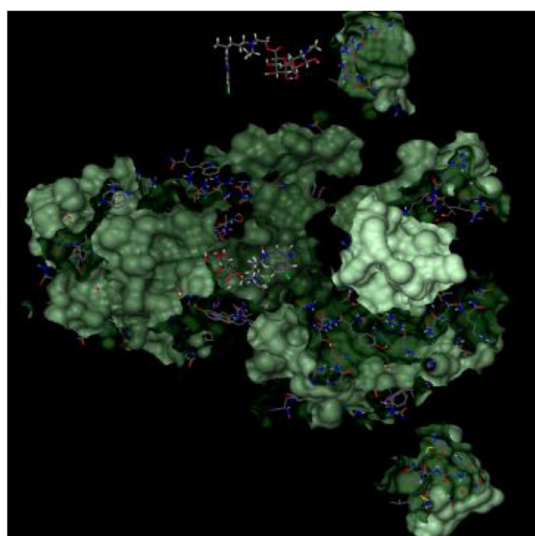
-13.6327 KJ/mol. It should be noted that HA-HCQ conjugate shows the highest binding affinity and docking score with SARS-CoV-2 viral target protein over HCQ (Table 3).

Among four COVID-19 protein targets, HA-HCQ conjugate possesses the highest binding affinity (-23.1778KJ/mol) with the crystal structure of helicase protein of COVID-19 (PDB ID 6ZSL) and it possesses 6 hydrogen bonds in that all 6 amino acid residues (Asp160,Tyr211,Gly213,Thr216,Tyr217,Glu341) of viral protein show both hydrogen and other noncovalent interactions with HA-HCQ conjugate. Whereas HCQ ligand shows binding affinity and docking score of -13.6327 KJ/mol with the crystal structure of the helicase protein of COVID-19 (PDB ID 6ZSL). It forms three hydrogen bonds with Lys192, Thr214 and Arg339 amino acid residues and it also has 11 non-covalent interactions between protein Helicase-HCQ ligand complexes.

The main protease of SARS-CoV-2 (PDB ID 5R82) shows higher binding affinity with HA-HCQ conjugate rather than with the HCQ and has docking scores of -22.4332 KJ/mol and -12.7873 KJ/mol respectively. The molecular interaction of HCQ and HA-HCQ drug conjugate forms hydrogen bond interaction with four (Ile152,



**a) Docking Pose and Interaction plot for 6ZSL-HCQ Complex (Binding Energy-13.6327KJ/mol)**



**b) Docking Pose and Interaction plot for 6ZSL-HA-HCQ Complex (Binding Energy-20.5752KJ/mol)**

**Fig. 5.** a & b - Docking Pose and Interaction for SARS-CoV-2 Helicase 6M71 with HCQ and HA-HCQ conjugate.

Tyr154, Val303, Thr304) and five (Leu141, Asn142, His164, Glu166, Gln189) amino acid residues of COVID-19 viral main protease respectively.

The HA-HCQ drug conjugate shows superior binding affinity of -19.2875 KJ/mol and -13.2046 KJ/mol with COVID-19 viral main protease molecular targets PDB ID 5R80 and PDB ID 6Y84 respectively than HCQ drug alone which shows docking scores of -11.2786 KJ/mol and -12.2217 KJ/mol. Moreover, HA-HCQ conjugate shows more number of hydrogen and non-covalent interactions with 5R80 and 6Y84 than the HCQ drug alone. It may be noted that some more hydrogen and noncovalent interactions are obtained through HA monomer conjugates to HCQ in all these two COVID-19 replications enzymes such as Mpro and Helicase further it assures and proves that hyaluronic acid (HA) will enhance the HCQ drug binding affinity towards viral target proteins.

The Hyaluronic acid (HA) is an important naturally occurring polysaccharide, virtually present in all extracellular matrixes of animal tissues. As CD44 is a primary hyaluronic acid receptor the

widespread type I transmembrane glycoprotein binds hyaluronic acid in most cell types. Moreover, CD44's standard isoform is virtually expressed in all cell types whereas its CD44 is expressed in few epithelial cells and cancers [29,30]. The present results prove that the target CD44 variant form of lower respiratory tract cells is the primary target replication site for SARS-CoV-2. The delivery of newly proposed HA-HCQ conjugates and its different degree of HCQ substitutions in HA will inhibit the viral replication cycle. It was established that HA-CD44 interactions play several essential role in cell adhesion, cell migration, cell survival, tumor cell proliferation, leukocyte trafficking and progression of inflammation [31-35].

The HA is predominately present throughout the body including lung tissue and shields the respiratory organ scleroprotein from inflammation [36,37]. The earlier scientific evidence confirms that HA is utilized in the distribution of drugs to the respiratory organ and also its sustained release of the drug makes

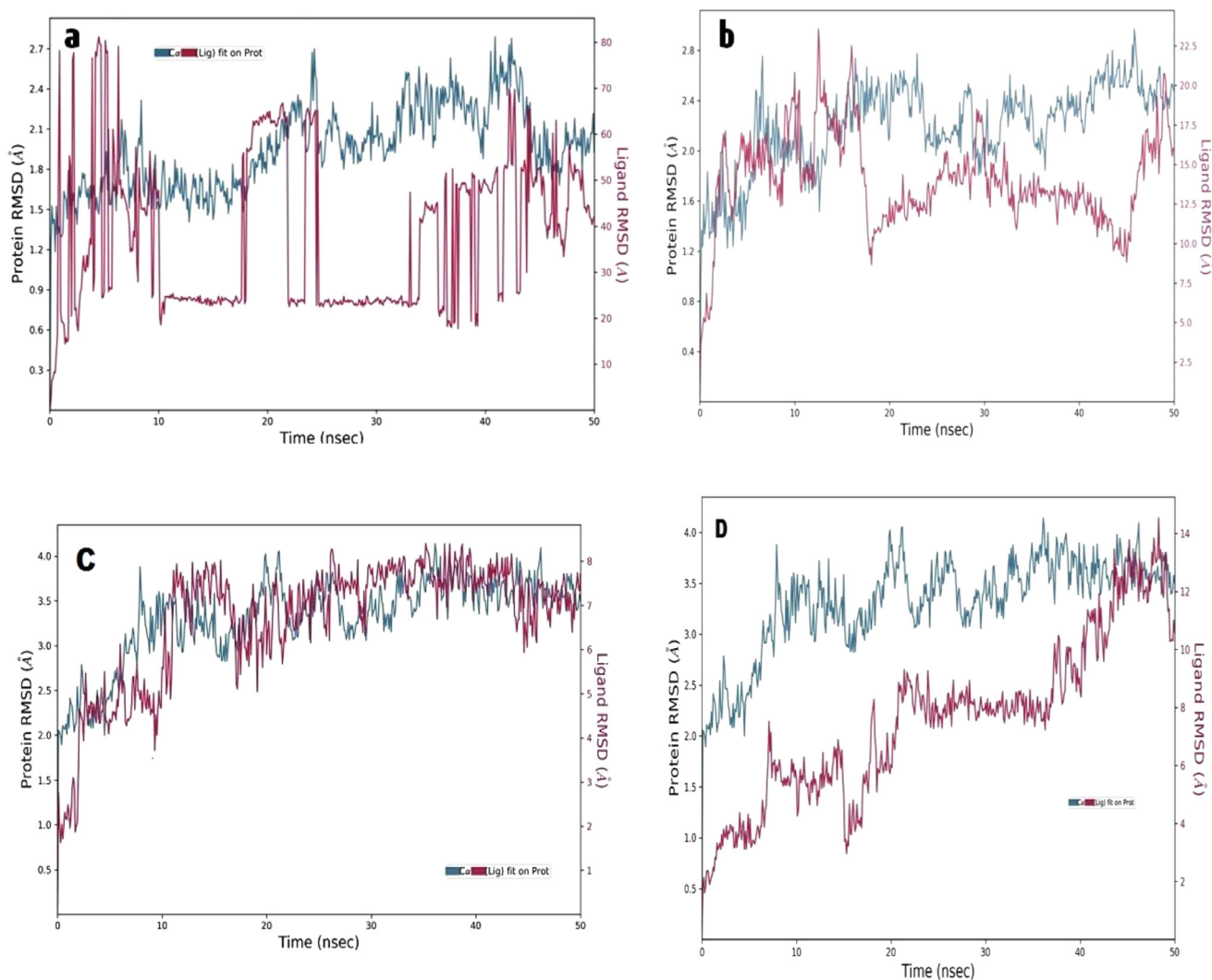


**Fig. 6.** RMSD of the Ca atoms of the target protein and the ligand over time. The left y-axis shows the variation in the target protein RMSD, and the right y-axis shows the variation in the ligand RMSD over time. (a) HCQ-Main protease (PDB ID 5R82) complex, (b) HAHQC-Main protease (PDB ID 5R82) complex, (c) HCQ-Helicase (PDB ID 6ZSL) complex (d) HAHQC-Helicase (PDB ID 6ZSL) complex.

biocompatibility, half-life extension, solubility enhancement, the possibility of high drug loading, less toxicity and increased drug retention time. Moreover, it is proposed that HA-HCQ drug conjugate enters into the lower respiratory tract cell through CD44 receptor, then under the influence of hydrolytic enzymes released from the lysosome, splits the HA-HCQ ester covalent bond and releases the HCQ drug into the target cell to interact with the SARS-COV-2 viral protein targets [37–39].

The degree of HCQ substitution on hyaluronic acid impact the uptake of HA-HCQ conjugates by CD44 variant isoforms of the lower respiratory tract. Another important way to increase the uptake of HA-HCQ conjugates by CD44 is through lipopolysaccharide (LPS) treatment. The interactions between hyaluronic acid and CD44 receptor is strictly regulated to maintain a quiescent state revealing little appreciable binding between them [40]. During inflammation, the pro-inflammatory cytokine such as TNF alpha induces sulfation and subsequent conformational changes in the CD44 receptor, which transforms it into a greater HA affinity [41]. Kamat et al. [42] reported the synthesis of iron oxide-based magnetic nanoparticles bearing hyaluronic acid on the surface to target activated macrophages. The low-molecular-weight of HA is a key player in macrophage activation, which could activate an innate immune response via Toll-Like Receptor TLR2 and TLR4 [43–45].

Moreover, earlier studies have proven that the delivery of drug rifampicin through a low degree of substitution of hyaluronic acid-Tocopherol succinate to alveolar macrophage cells. Further, these RIF-HA-TS conjugate shows enhanced interaction with CD44 receptor that leads to the entry of drug-conjugate complex inside the MH-S murine alveolar macrophage cells [46].

Hydroxychloroquine (HCQ) is an anti-malarial drug that shows its efficiency by saving millions of lives during the COVID-19 outbreak. Chloroquine is a versatile bioactive agent that possess antiviral action against numerous RNA viruses such as HIV [47–49], Hepatitis A virus [50,51], Hepatitis C virus [52], Poliovirus [53], Rabies virus [54], Influenza A & B virus [55–58], SARS-CoV-1 [59]. It also inhibits in vitro replication of HCoV-229E [60] and also found to inhibit MERS-CoV [61] in in vitro condition. The HCQ is a fairly safe drug and offer potentially useful treatment options for COVID-19 disease of the respiratory tract. Hydroxychloroquine has been known to possess in vitro anti-SARS-CoV effect. The prolonged usage of the clinical safety profile of Hydroxychloroquine is greater than that of Chloroquine for prolonged usage of drugs and makes a higher daily dose and has fewer questions regarding drug-drug interactions [62].

The HCQ anti-viral mechanism such as inhibition of viral attachment and entry into the host cell, inhibition of N-glycosylation

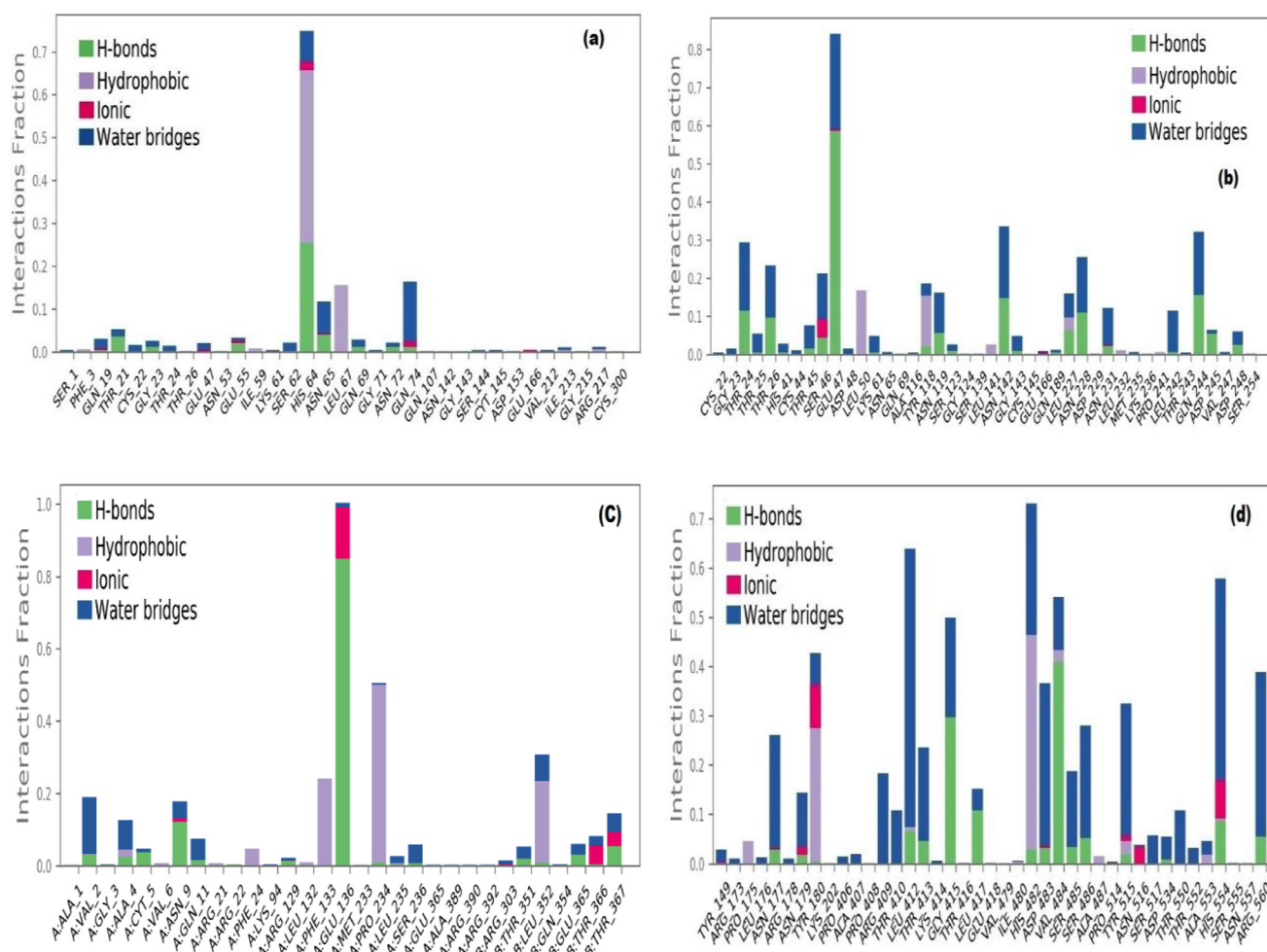


**Fig. 7.** Protein-Ligand Interactions (a) HCQ-Main protease (PDB ID 5R82) complex, (b) HA-HCQ-Main protease (PDB ID 5R82) complex, (c) HCQ-Helicase (PDB ID 6ZSL) complex (d) HA-HCQ-Helicase (PDB ID 6ZSL) complex.

of cell surface viral receptor ACE2 [63,64], inhibition of N-glycosylation of viral spike protein [65], endosomal alkalization [66], inhibition of phospholipase A2 and membranous structure are essential for replication and translation of viral particles [67]. The HCQ also possess immunosuppressive properties that may help to reduce the cytokine storm in severe COVID-19 [68,69].

### 3.3. Molecular dynamics (MD) and simulation

The MD simulation was performed for four complexes HCQ-Mpro (PDB ID 5R82), HAHCQ-Mpro (PDB ID 5R82), HCQ-Helicase (PDB ID 6ZSL) and HAHCQ-Helicase (PDB ID 6ZSL) at 50 ns and their results are presented in Figs. 6–9. The RMSD plots show the RMSD evolution of a protein (left Y-axis). All protein frames are first aligned on the reference frame backbone, and then the RMSD is calculated based on the atom selection. Monitoring the RMSD of the protein can give insights into its structural conformation throughout the simulation. The RMSD analysis can indicate if the simulation has equilibrated - its fluctuations towards the end of the simulation are around some thermal average structure. The Ligand RMSD (right Y-axis) indicates how stable the ligand is concerning the protein and its binding pocket. This plot, 'Lig fit Prot' shows the RMSD of a ligand when the protein-ligand complex is first aligned on the protein backbone of the reference and then the RMSD of the ligand heavy atoms is measured.

The HA-HCQ-Mpro (PDB ID 5R82) RMSD (root mean square deviation) plot shows that both HA-HCQ conjugate and Mpro (PDB

ID 5R82) are stable for the first 20 ns at 2.4 Å for ligand and 2.0 Å for protein. A slight deviation of protein structure can be observed after 20 ns. This plot shows that by the end of the simulation, the ligand structures were found to be stable at 2.2 Å after 45 ns but proteins were undergoing continuous conformational changes and they might need longer simulation to be stable because of their large structure (Fig. 6b) whereas HCQ-Mpro (PDB ID 5R82) complex shown stable at 1.8 Å from 1–10 ns and 45–50 ns (Fig. 6a). The changes in the order 1–3 Å is perfectly acceptable for small and globular shape proteins. The HAHCQ-Helicase (PDB ID 6ZSL) complex (Fig. 6d) shows stability after 45 ns at 3.0 Å. A slight deviation from 1.5 Å to 2.0 Å happened up to 30 ns whereas HCQ-Helicase (PDB ID 6ZSL) complex has shown stable at 3.5 Å from 1–50 ns (Fig. 6c). The HAHCQ-Mpro (PDB ID 5R82) complex shows the high level of interaction throughout the simulation. It may be observed that HA-HCQ-Mpro (PDB ID 5R82) structures are continuously interacting at the same deviation rate and showing less deviation in the structures. The HA-HCQ-Mpro (PDB ID 5R82) structures seemed to be stable for most of the time of the simulation.

The study of stable ligand-protein interactions and the contribution of specific residues to ligand binding in the pocket is an important aspect of the detection of hotspots. From the results of molecular dynamics simulation, it was observed that Mpro (PDB ID 5R82) residues THR24, THR26 and GLU47, ASN142, ASN228 and GLN244 possess the highest interaction fractions value of 0.25 with HA-HCQ conjugate whereas HCQ ligand shows an interaction frac-

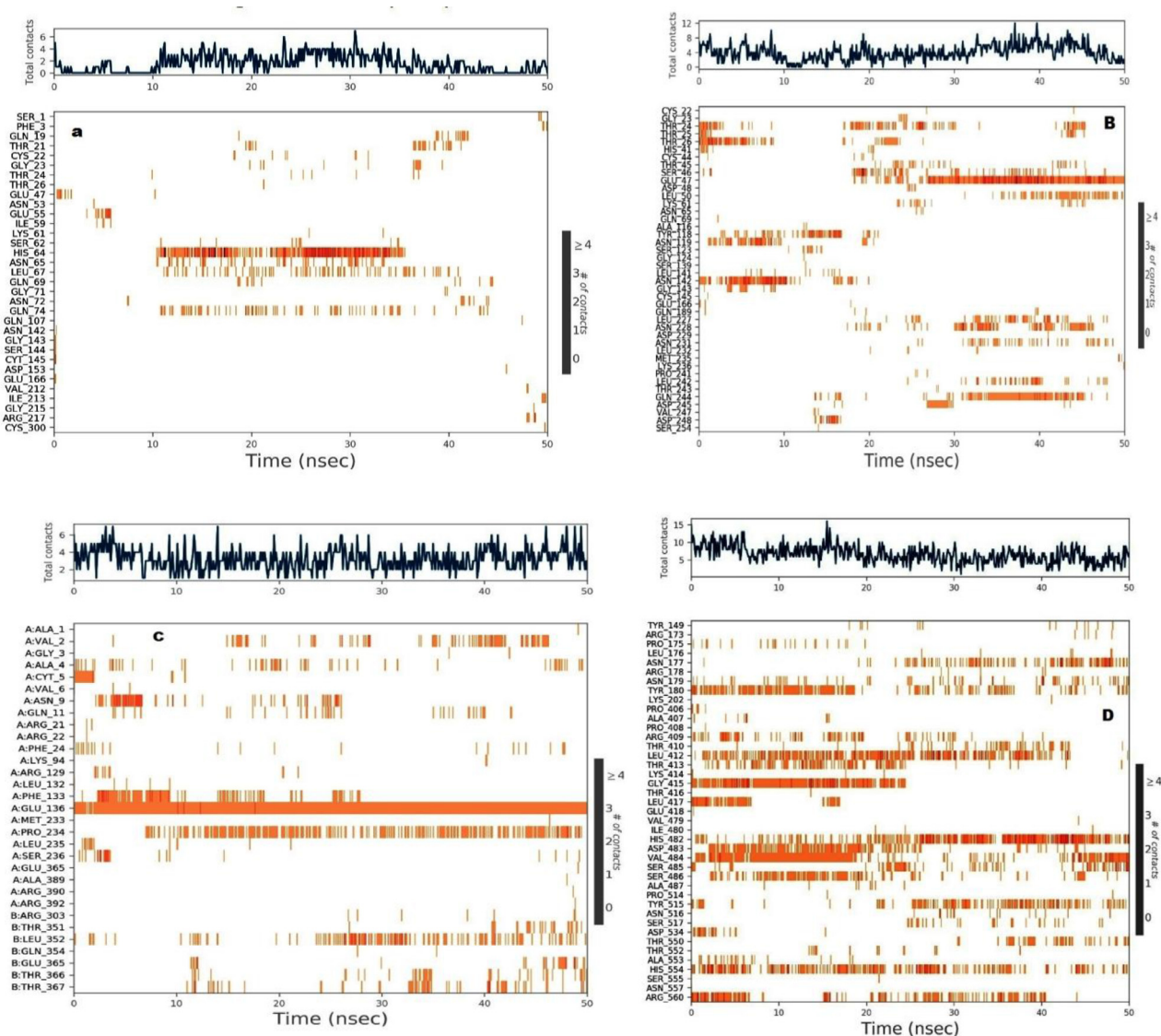


**Fig. 8.** Timeline representation of the interactions and contacts (H-bonds, Hydrophobic, Ionic, and Water bridges) the top panel of each image shows the total number of specific contacts the protein makes with the ligand throughout the trajectory. The bottom panel of each image shows which residues interact with the ligand in each trajectory frame. (a) HCQ-Main protease (PDB ID 5R82) complex, (b) HAHCQ-Main protease (PDB ID 5R82) complex, (c) HCQ-Helicase (PDB ID 6ZSL) complex (d) HAHCQ-Helicase (PDB ID 6ZSL) complex.

tion of 0.25 with one residue HIS64 of Mpro (Fig. 7 a & b). Helicase 6ZSL residues TYR 180, LEU412, THR415, ASP482, VAL483, SER484, TYR515, HIS554 and ARG560 possess 0.3 to 0.7 interaction fraction values with HA-HCQ conjugate whereas HCQ has 0.3 interaction fraction values only with three residues i.e. GLU136, PRO234 and LEU352 of Helicase (PDB ID 6ZSL) during the span of simulation (Fig. 7 c & d). HA-HCQ-Mpro (PDB ID 5R82) and HA-HCQ-Helicase (PDB ID 6ZSL) complexes show the prominent number of amino acid residues with different types of interaction including hydrophobic bonds, ionic bonds and water bridges bonds. The Protein and ligands timeline interaction graph show a high amount of interaction for HA-HCQ-Mpro5R82 complex (Fig. 8b), and HA-HCQ- Helicase (PDB ID 6ZSL) complex (Fig. 8d). These results confirm the promising effects of HA-HCQ on the target proteins of SARS-CoV-2. The Residue-wise RMSF values of the SARS-CoV-2 Mpro (PDB ID 5R82) and Helicase (PDB ID 6ZSL) proteins bound to HA and HA-HCQ conjugates during the simulations were presented in Fig. 9 (a-d). They also depict atom-wise RMSF of the ligand concerning its corresponding receptors. It is apparent from these results that for all the complexes, during triplicate simula-

tions, most of the amino acid residues have an RMSF value  $<2.0 \text{ \AA}$  and most HA-HCQ conjugate atoms whereas HCQ possess RMSF value  $<1.5 \text{ \AA}$ .

Recently, Kumar et al., 2020 [70] reported the MD simulation results of Noscapine-Hydroxychloroquine (Nos-HCQ) conjugates. The authors showed strong binding affinity for the main protease (Mpro) of SARS-CoV-2, which performs key biological function in virus infection and progression. Further, MD simulation study of Nos-HCQ affirmed the stable binding of the conjugate to Mpro domains and possesses unprecedented results of RMSD, complex dynamics and radius of gyration plots along with critical reaction coordinate binding free energy profile. Nabajyoti et al., 2020 [71] also reported that Hydroxychloroquine possesses a high docking score and interaction energies and a decent level of docking within the cavity in the main protease moiety of SARS-CoV-2. Molecular dynamics simulations lead to the evaluation of conformational energies, average H-bonding distance, RMSD plots etc. Large RMSD fluctuations for the first 2 ns seem to provide the conformational and rotational changes associated with the drug molecule when it comes into the vicinity of the

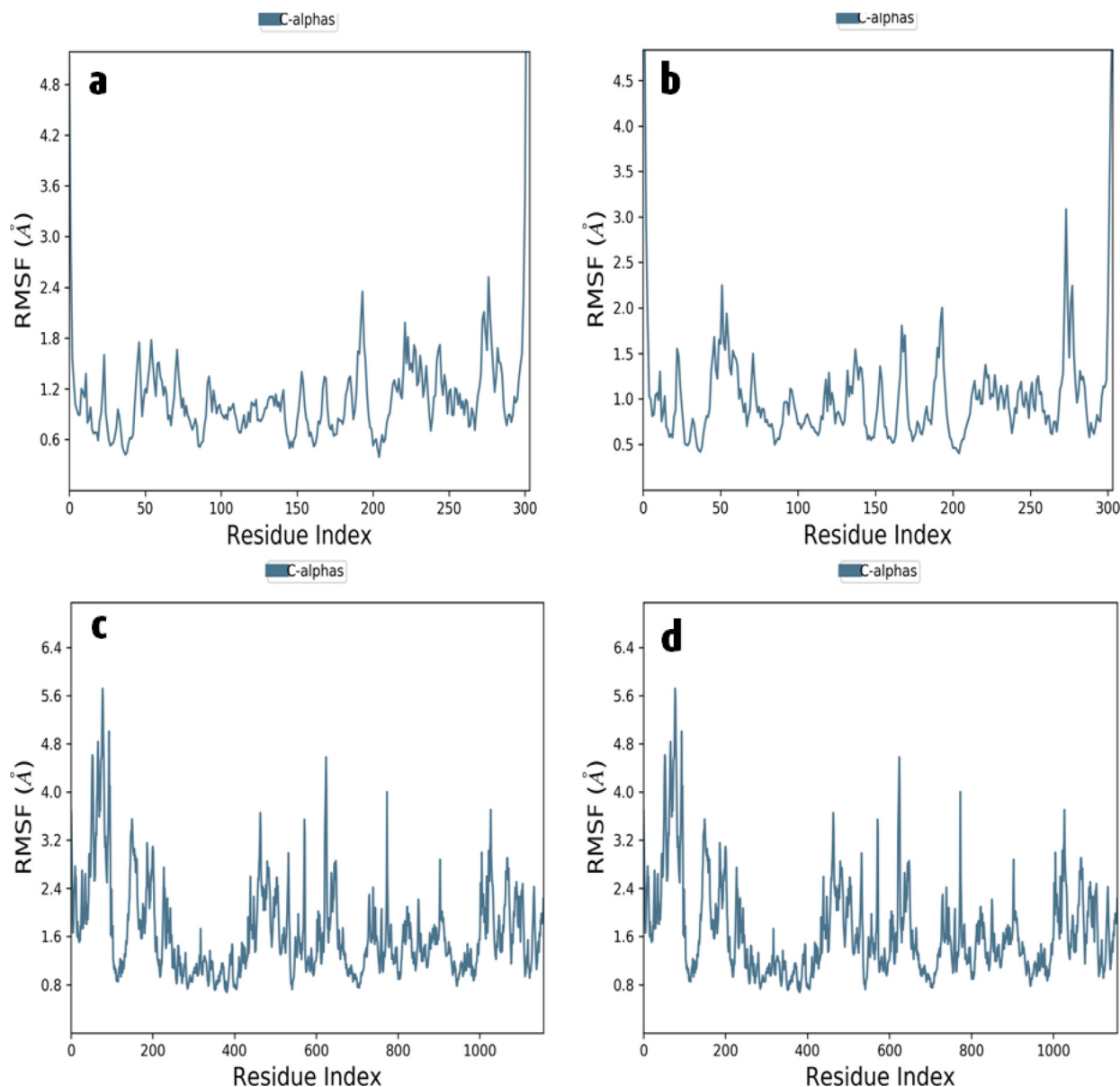


**Fig. 9.** Residue-wise RMSF of ligand concerning receptor protein during triplicate simulations (a) HCQ-Main protease (PDB ID 5R82) complex, (b) HAHCQ-Main protease (PDB ID 5R82) complex, (c) HCQ-Helicase (PDB ID 6ZSL) complex (d) HAHCQ-Helicase (PDB ID 6ZSL) complex.

protease matrix. Finally, the present docking and MD simulation study provide good insight to the HA-HCQ conjugate possesses good and stable binding affinity with binding pockets of Mpro and helicase proteins of SARS-CoV-2, which pave the way for further in vitro and in vivo examination of HA-HCQ drug conjugate with robust binding against Mpro and helicase protein targets of SARS-CoV-2.

#### 4. Conclusion

The molecular docking study was used to evaluate the safety of drug delivery, targeting receptors, toxicity, solubility and efficacy of Hyaluronic acid-Hydroxychloroquine (HA-HCQ) conjugate over free Hydroxychloroquine (HCQ) drug. Four SARS-CoV-2 viral molecular protein targets have been analyzed with HA-HCQ and the results obtained reveal better interactions with viral protein targets than the free HCQ drug. The HA-HCQ drug conjugate showed maximal drug delivery to lower respiratory tract through CD44 receptors with increased drug clearance and less toxicity to host cells.

The results of MD simulation trajectories study reveal that HA-HCQ-SARS-CoV-2 protein complexes found superior complex stability over HCQ- SARS-CoV-2 protein complexes. Further studies are in progress to the synthesis of HA-HCQ conjugates with different degrees of substitutions of drugs to the polymer and to evaluate the antiviral activity both in *in-vitro* and *in-vivo* towards Mpro and Helicase SAR-CoV-2 viral protein targets. This will leads to the establishment of a promising and novel treatment option for COVID-19 and other related diseases through its versatile drug conjugation technology.

#### Authors' contribution

Conception and design of study: Riaz Khan, V. Aroulmoji, C. Sivasankar

Acquisition of data: R. Thirumalaisamy, Muhammad Nasir Iqbal, T.Selvankumar

Analysis and/or interpretation of data: T.Selvankumar, R. Thirumalaisamy, Riaz Khan

Drafting the manuscript: R. Thirumalaisamy, Riaz Khan, V. Aroulmoji

Revising the manuscript critically for important intellectual content: Riaz Khan, M. Deepa, C. Sivasankar

Approval of the version of the manuscript to be published (the names of all authors must be listed): R. Thirumalaisamy, V. Aroulmoji, Muhammad Nasir Iqbal, M. Deepa, C. Sivasankar, Riaz Khan, T. Selvankumar

## Declaration of Competing Interest

None.

## References

- [1] L. Alanagreh, F. Alzoughool, M. Atoum, Risk of using hydroxychloroquine as a treatment of COVID-19, *Int. J. Risk Saf. Med.* 31 (2020) 111–116, doi:10.3233/JRS-200024.
- [2] D.J. Morris, Adverse effects and drug interactions of clinical importance with antiviral drugs, *Drug Saf.* 10 (1994) 281–291, doi:10.2165/00002018-199410040-00002.
- [3] Stefano Norbedo, Susanna Bosi, Massimo Bergamin, Riaz Ahmed Khan, Ermínio Murano, Use of hyaluronic acid as a carrier molecule for different classes of therapeutic active agents, WO/2007/085629, EP1976539, US20090197797, CN101374531, CA2640159, AU2007209366, JP2009524624, IN4408/CHENP/2008
- [4] R. Khan, B. Mahendhiran, V. Aroulmoji, Chemistry of hyaluronic acid and its significance in drug delivery strategies: a review, *Int. J. Pharm. Sci. Res.* 4 (2013) 3699–3710, doi:10.13040/IJPSR.0975-8232.4(10).3699-10.
- [5] R. Khan, V. Aroulmoji, Hyaluronic acid - hydroxychloroquine conjugate proposed for treatment of COVID-19, *Int. J. Adv. Sci. Eng.* 6 (4) (2020) 1469–1471, doi:10.29294/IJASE.6.4.2020.1469-1471.
- [6] E.A. Turley, P.W. Noble, L.Y.W. Bourguignon, Signaling properties of hyaluronan receptors, *J. Biol. Chem.* 277 (2002) 4589–4592, doi:10.1074/jbc.R100038200.
- [7] Y. Gouffé, C. Guilluy, P. Guérin, P. Patra, P. Pacaud, G. Loirand, Hyaluronan induces vascular smooth muscle cell migration through RHAMM-mediated PI3K-dependent Rac activation, *Cardiovasc. Res.* 72 (2006) 339–348, doi:10.1016/j.cardiores.2006.07.017.
- [8] S.V. Kyosseva, E.N. Harris, P.H. Weigel, The hyaluronan receptor for endocytosis mediates hyaluronan-dependent signal transduction via extracellular signal-regulated kinases, *J. Biol. Chem.* 283 (2008) 15047–15055, doi:10.1074/jbc.M709921200.
- [9] C.A. Maxwell, J. McCarthy, E. Turley, Cell-surface and mitotic-spindle RHAMM: moonlighting or dual oncogenic functions? *J. Cell Sci.* 121 (2008) 925–932, doi:10.1242/jcs.022038.
- [10] W. Knudson, R.S. Peterson, The hyaluronan receptor: CD44, *Chem. Biol. Hyaluronan.* 298 (2004) 83–123, doi:10.1016/B978-0-08044382-9/50036-4.
- [11] M.S. Pandey, P.H. Weigel, Hyaluronic acid receptor for endocytosis (HARE)-mediated endocytosis of hyaluronan, heparin, dermatan sulfate, and acetylated low density lipoprotein (AcLDL), but not chondroitin sulfate types A, C, D, or E, activates NF- $\kappa$ B-regulated gene expression, *J. Biol. Chem.* 289 (2014) 1756–1767, doi:10.1074/jbc.M113.510339.
- [12] D. Park, Y. Kim, H. Kim, K. Kim, Y.S. Lee, J. Choe, J.H. Hahn, H. Lee, J. Jeon, C. Choi, Y.M. Kim, D. Jeong, Hyaluronic acid promotes angiogenesis by inducing RHAMM-TGF $\beta$  receptor interaction via CD44-PKC $\delta$ , *Mol. Cells* 33 (2012) 563–574, doi:10.1007/s10059-012-2294-1.
- [13] W. Lawrence, S. Banerji, A.J. Day, S. Bhattacharjee, D.G. Jackson, Binding of hyaluronan to the native lymphatic vessel endothelial receptor LYVE-1 is critically dependent on receptor clustering and hyaluronan organization, *J. Biol. Chem.* 291 (2016) 8014–8030, doi:10.1074/jbc.M115.708305.
- [14] C. Sorbi, M. Bergamin, S. Bosi, F. Dinon, V. Aroulmoji, R. Khan, E. Murano, S. Norbedo, Synthesis of 6-O-methoxyhyaluronan as a drug delivery system, *Carbohydr. Res.* 344 (2009) 91–97, doi:10.1016/j.carres.2008.09.021.
- [15] Riaz Khan and A. Paul Konowicz, A: Dicarboxylic acid hemiester or hemiamide with a pharmacologically active compound and with hyaluronic acid or with a hyaluronic acid ester, a process for its preparation and a controlled release medicament containing this derivative: WO1996035721 A1 (1996). <https://patents.google.com/patent/WO1996035721A1/de>
- [16] P. Gautret, J.C. Lagier, P. Parola, V.T. Hoang, L. Meddeb, M. Mailhe, B. Doudier, J. Courjon, V. Giordanengo, V.E. Vieira, H. Tissot Dupont, S. Honoré, P. Colson, E. Chabrière, B. La Scola, J.M. Rolain, P. Brouqui, D. Raoult, Hydroxychloroquine and azithromycin as a treatment of COVID-19: results of an open-label non-randomized clinical trial, *Int. J. Antimicrob. Agents* 56 (2020) 105949, doi:10.1016/j.ijantimicag.2020.105949.
- [17] G.K. Helal, M.A. Gad, M.F. Abd-Ellah, M.S. Eid, Hydroxychloroquine augments early virological response to pegylated interferon plus ribavirin in genotype-4 chronic hepatitis C patients, *J. Med. Virol.* 88 (2016) 2170–2178, doi:10.1002/jmv.24575.
- [18] K. Sperber, M. Louie, T. Kraus, J. Pröner, E. Sapira, S. Lin, V. Stecher, L. Mayer, Hydroxychloroquine treatment of patients with human immunodeficiency virus type 1, *Clin. Ther.* 17 (1995) 622–636, doi:10.1016/0149-2918(95)80039-5.
- [19] X. Yao, F. Ye, M. Zhang, C. Cui, B. Huang, P. Niu, L. Zhao, E. Dong, C. Song, S. Zhan, R. Lu, H. Li, D. Liu, D. Clinical, D. Liu, W. Tan, D. Clinical, In vitro antiviral activity and projection of optimized dosing design of hydroxychloroquine for the treatment of severe acute respiratory syndrome main point : hydroxychloroquine was found to be more potent than chloroquine at inhibiting SARS-CoV-2 in vit, *Clin. Infect. Dis.* 2 (2020) 1–25, doi:10.1093/cid/ciaa237.
- [20] K. Sperber, G. Chiang, H. Chen, W. Ross, E. Chusid, M. Gonchar, R. Chow, O. Liriano, Comparison of hydroxychloroquine with zidovudine in asymptomatic patients infected with human immunodeficiency virus type 1, *Clin. Ther.* 19 (1997) 913–923, doi:10.1016/S0149-2918(97)80045-8.
- [21] P. Mehta, D.F. McAuley, M. Brown, E. Sanchez, R.S. Tattersall, J.J. Manson, COVID-19: consider cytokine storm syndromes and immunosuppression, *Lancet* 395 (2020) 1033–1034, doi:10.1016/S0140-6736(20)30628-0.
- [22] T. Rathinavel, M. Arts, G. Shanmugam, In silico validation of phytochemicals from *Cratogeomys adansonii* against multiple targets of inflammation in silico validation of phytochemicals from *Cratogeomys adansonii* against multiple targets of inflammation, 6 (2018) 6–16.
- [23] D. Weininger, SMILES, a chemical language and information system: 1: introduction to methodology and encoding rules, *J. Chem. Inf. Comput. Sci.* 28 (1988) 31–36, doi:10.1021/ci00057a005.
- [24] H.M. Berman, T. Battistuz, T.N. Bhat, W.F. Bluhm, P.E. Bourne, K. Burkhardt, Z. Feng, G.L. Gilliland, L. Iype, S. Jain, P. Fagan, J. Marvin, D. Padilla, V. Ravichandran, B. Schneider, N. Thanki, H. Weissig, J.D. Westbrook, C. Zardecki, The protein data bank, *Acta Crystallogr. Sect. D Biol. Crystallogr.* 58 (2002) 899–907, doi:10.1107/S0907444902003451.
- [25] M. Rarey, B. Kramer, T. Lengauer, G. Klebe, A fast flexible docking method using an incremental construction algorithm, *J. Mol. Biol.* 261 (1996) 470–489, doi:10.1006/jmbi.1996.0477.
- [26] K. Stierand, P.C. Maaß, M. Rarey, Molecular complexes at a glance: automated generation of two-dimensional complex diagrams, *Bioinformatics* 22 (2006) 1710–1716, doi:10.1093/bioinformatics/btl150.
- [27] D.E. Shaw, R.O. Dror, J.K. Salmon, J.P. Grossman, K.M. MacKenzie, J.A. Bank, C. Young, M.M. Deneroff, B. Batson, K.J. Bowers, E. Chow, M.P. Eastwood, D.J. Lerardi, J.L. Klepeis, J.S. Kuskin, R.H. Larson, K. Lindorff-Larsen, P. Maragakis, M.A. Moraes, S. Piana, Y. Shan, B. Towles, Millisecond-scale molecular dynamics simulations on Anton, in: *Proc. Conf. High Perform. Comput. Networking, Storage Anal. SC '09*, 2009, pp. 1–11, doi:10.1145/1654059.1654099.
- [28] G. Madhavi Sastry, M. Adzhigirey, T. Day, R. Annabhimoju, W. Sherman, Protein and ligand preparation: parameters, protocols, and influence on virtual screening enrichments, *J. Comput. Aided. Mol. Des.* 27 (2013) 221–234, doi:10.1007/s10822-013-9644-8.
- [29] D. Shivakumar, J. Williams, Y. Wu, W. Damm, J. Shelley, W. Sherman, Prediction of absolute solvation free energies using molecular dynamics free energy perturbation and the opls force field, *J. Chem. Theory Comput.* 6 (2010) 1509–1519, doi:10.1021/ct900587b.
- [30] A. Subash, G. Veeraraghavan, V.K. Sali, M. Bhardwaj, H.R. Vasanthi, Attenuation of inflammation by marine algae *Turbinaria ornata* in cotton pellet induced granuloma mediated by fucoidan like sulphated polysaccharide, *Carbohydr. Polym.* 151 (2016) 1261–1268, doi:10.1016/j.carbpol.2016.06.077.
- [31] J.P. Sleeman, K. Kondo, J. Moll, H. Ponta, P. Herrlich, Variant exons v6 and v7 together expand the repertoire of glycosaminoglycans bound by CD44, *J. Biol. Chem.* 272 (1997) 31837–31844, doi:10.1074/jbc.272.50.31837.
- [32] H. Ponta, L. Sherman, P.A. Herrlich, CD44: from adhesion molecules to signalling regulators, *Nat. Rev. Mol. Cell Biol.* 4 (2003) 33–45, doi:10.1038/nrm1004.
- [33] B.P. Toole, T.N. Wight, M.I. Tammi, Hyaluronan-cell interactions in cancer and vascular disease, *J. Biol. Chem.* 277 (2002) 4593–4596, doi:10.1074/jbc.R100039200.
- [34] S. Misra, P. Heldin, V.C. Hascall, N.K. Karamanos, S.S. Skandalis, R.R. Markwald, S. Ghatak, Hyaluronan-CD44 interactions as potential targets for cancer therapy, *FEBS J.* 278 (2011) 1429–1443, doi:10.1111/j.1742-4658.2011.08071.x.
- [35] S. Misra, S. Ghatak, A. Zoltan-Jones, B.P. Toole, Regulation of multidrug resistance in cancer cells by hyaluronan, *J. Biol. Chem.* 278 (2003) 25285–25288, doi:10.1074/jbc.C300173200.
- [36] D. Bhattacharya, D. Svehkarev, J.J. Souček, T.K. Hill, M.A. Taylor, A. Nataraajan, A.M. Mohs, A. Diseases, P. Buffett, HHS Public Access 5 (2018) 8183–8192, doi:10.1039/C7TB01895A.Impact.
- [37] K. Konno, H. Arai, M. Motomiya, H. Nagai, M. Ito, H. Sato, K. Satoh, A biochemical study on glycosaminoglycans (mucopolysaccharides) in emphysematous and in aged lungs, *Am. Rev. Respir. Dis.* 126 (1982) 797–801, doi:10.1164/arrd.1982.126.5.797.
- [38] S. Norbedo, F. Dinon, M. Bergamin, S. Bosi, V. Aroulmoji, R. Khan, E. Murano, Synthesis of 6-amino-6-deoxyhyaluronan as an intermediate for conjugation with carboxylate-containing compounds: application to hyaluronan-campothecin conjugates, *Carbohydr. Res.* 344 (2009) 98–104, doi:10.1016/j.carres.2008.09.027.
- [39] F. Marchetti, A. Fallacara, M. Pozzoli, U.R. Citernesi, S. Manfredini, S. Vertuani, Formulation and characterization of native and crosslinked hyaluronic acid microspheres for dermal delivery of sodium ascorbyl phosphate: a comparative study, *Pharmaceutics* 10 (2018), doi:10.3390/pharmaceutics10040254.
- [40] A. Nandi, P. Estess, M.H. Siegelman, Hyaluronan anchoring and regulation on the surface of vascular endothelial cells is mediated through the functionally active form of CD44, *J. Biol. Chem.* 275 (2000) 14939–14948, doi:10.1074/jbc.275.20.14939.
- [41] K. Gee, M. Kozłowski, M. Kryworuchko, F. Diaz-Mitoma, A. Kumar, Differential effect of IL-4 and IL-13 on CD44 expression in the Burkitt's lymphoma

- B cell line BL30/B95-8 and in Epstein-Barr virus (EBV) transformed human B cells: loss of IL-13 receptors on Burkitt's lymphoma B cells, *Cell. Immunol.* 211 (2001) 131–142, doi:[10.1006/cimm.2001.1829](https://doi.org/10.1006/cimm.2001.1829).
- [42] M. Kamat, K. El-Boubbou, D.C. Zhu, T. Lansdell, X. Lu, W. Li, X. Huang, Hyaluronic acid immobilized magnetic nanoparticles for active targeting and imaging of macrophages, *Bioconjug. Chem.* 21 (2010) 2128–2135, doi:[10.1021/bc100354m](https://doi.org/10.1021/bc100354m).
- [43] J. Muto, K. Yamasaki, K.R. Taylor, R.L. Gallo, Engagement of CD44 by hyaluronan suppresses TLR4 signaling and the septic response to LPS, *Mol. Immunol.* 47 (2009) 449–456, doi:[10.1016/j.molimm.2009.08.026](https://doi.org/10.1016/j.molimm.2009.08.026).
- [44] C.M. McKee, M.B. Penno, M. Cowman, M.D. Burdick, R.M. Strieter, C. Bao, P.W. Noble, Hyaluronan (HA) fragments induce chemokine gene expression in alveolar macrophages: The role of HA size and CD44, *J. Clin. Invest.* 98 (1996) 2403–2413, doi:[10.1172/JCI119054](https://doi.org/10.1172/JCI119054).
- [45] Y. Gao, M.K. Sarfraz, S.D. Clas, W. Roa, R. Löbenberg, Hyaluronic acid-tocopherol succinate-based self-assembling micelles for targeted delivery of rifampicin to alveolar macrophages, *J. Biomed. Nanotechnol.* 11 (2014) 1312–1329, doi:[10.1166/jbnn.2015.2091](https://doi.org/10.1166/jbnn.2015.2091).
- [46] M. Million, J.C. Lagier, P. Gautret, P. Colson, P.E. Fournier, S. Amrane, M. Hocquart, M. Mailhe, V. Esteves-Vieira, B. Doudier, C. Aubry, F. Correard, A. Giraud-Gatineau, Y. Roussel, C. Berenger, N. Cassir, P. Seng, C. Zandotti, C. Dhiver, I. Ravoux, C. Tomei, C. Eldin, H. Tissot-Dupont, S. Honoré, A. Stein, A. Jacquier, J.C. Deharo, E. Chabrière, A. Lévassieur, F. Fenollar, J.M. Rolain, Y. Obadia, P. Brouqui, M. Drancourt, B. La Scola, P. Parola, D. Raoult, Early treatment of COVID-19 patients with hydroxychloroquine and azithromycin: a retrospective analysis of 1061 cases in Marseille, France, *Travel Med. Infect. Dis.* 35 (2020) 101738, doi:[10.1016/j.tmaid.2020.101738](https://doi.org/10.1016/j.tmaid.2020.101738).
- [47] W. po Tsai, P.L. Nara, H. fu Kung, S. Oroszlan, Inhibition of human immunodeficiency virus infectivity by chloroquine, *AIDS Res. Hum. Retroviruses* 6 (1990) 481–489, doi:[10.1089/aid.1990.6.481](https://doi.org/10.1089/aid.1990.6.481).
- [48] L. Gennero A. Savarino, K. Sperber, J.R. Boelaert, The anti-HIV-1 activity of chloroquine, *J. Clin. Virol.* 20 (2001) 131–135, doi:[10.1016/S1386-6532\(00\)00139-6](https://doi.org/10.1016/S1386-6532(00)00139-6).
- [49] F. Romanelli, K. Smith, A. Hoven, Chloroquine and Hydroxychloroquine as Inhibitors of Human Immunodeficiency Virus (HIV-1) activity, *Curr. Pharm. Des.* 10 (2005) 2643–2648, doi:[10.2174/1381612043383791](https://doi.org/10.2174/1381612043383791).
- [50] F. Superti, L. Seganti, N. Orsi, M. Divizia, R. Gabrieli, A. Panà, The effect of lipophilic amines on the growth of hepatitis A virus in Frp/3 cells, *Arch. Virol.* 96 (1987) 289–296, doi:[10.1007/BF01320970](https://doi.org/10.1007/BF01320970).
- [51] N.E. Bishop, Examination of potential inhibitors of hepatitis A virus uncoating, *Intervirology* 41 (1998) 261–271, doi:[10.1159/000024948](https://doi.org/10.1159/000024948).
- [52] T. Mizui, S. Yamashina, I. Tanida, Y. Takei, T. Ueno, N. Sakamoto, K. Ikejima, T. Kitamura, N. Enomoto, T. Sakai, E. Kominami, S. Watanabe, Inhibition of hepatitis C virus replication by chloroquine targeting virus-associated autophagy, *J. Gastroenterol.* 45 (2010) 195–203, doi:[10.1007/s00535-009-0132-9](https://doi.org/10.1007/s00535-009-0132-9).
- [53] P. Kronenberger, R. Vrijns, A. Boeyé, Chloroquine induces empty capsid formation during poliovirus eclipse, *J. Virol.* 65 (1991) 7008–7011, doi:[10.1128/jvi.65.12.7008-7011.1991](https://doi.org/10.1128/jvi.65.12.7008-7011.1991).
- [54] M.H.V. Van Regenmortel, *Archives of virology: editorial*, *Arch. Virol.* 144 (1999) 377–382.
- [55] D.K. Miller, J. Lenard, Antihistaminics, local anesthetics, and other amines as antiviral agents, *Proc. Natl. Acad. Sci. USA* 78 (1981) 3605–3609, doi:[10.1073/pnas.78.6.3605](https://doi.org/10.1073/pnas.78.6.3605).
- [56] M. Shibata, H. Aoki, T. Tsurumi, Y. Sugiura, Y. Nishiyama, S. Suzuki, K. Maeno, Mechanism of uncoating of influenza B virus in MDCK cells: Action of chloroquine, *J. Gen. Virol.* 64 (1983) 1149–1156, doi:[10.1099/0022-1317-64-5-1149](https://doi.org/10.1099/0022-1317-64-5-1149).
- [57] E.O. Eng, J.S.W. Chew, P.L. Jin, R.C.S. Chua, In vitro inhibition of human influenza A virus replication by chloroquine, *Virol. J.* 3 (2006) 3–5, doi:[10.1186/1743-422X-3-39](https://doi.org/10.1186/1743-422X-3-39).
- [58] N.I. Paton, L. Lee, Y. Xu, E.E. Ooi, Y.B. Cheung, S. Archuleta, G. Wong, A.W. Smith, Chloroquine for influenza prevention: a randomised, double-blind, placebo controlled trial, *Lancet Infect. Dis.* 11 (2011) 677–683, doi:[10.1016/S1473-3099\(11\)70065-2](https://doi.org/10.1016/S1473-3099(11)70065-2).
- [59] E. Keyaerts, S. Li, L. Vijgen, E. Rysman, J. Verbeeck, M. Van Ranst, P. Maes, Antiviral activity of chloroquine against human coronavirus OC43 infection in newborn mice, *Antimicrob. Agents Chemother.* 53 (2009) 3416–3421, doi:[10.1128/AAC.01509-08](https://doi.org/10.1128/AAC.01509-08).
- [60] M. Kono, K. Tatsumi, A.M. Imai, K. Saito, T. Kuriyama, H. Shirasawa, Inhibition of human coronavirus 229E infection in human epithelial lung cells (L132) by chloroquine: Involvement of p38 MAPK and ERK, *Antiviral Res.* 77 (2008) 150–152, doi:[10.1016/j.antiviral.2007.10.011](https://doi.org/10.1016/j.antiviral.2007.10.011).
- [61] Y. Mo, D. Fisher, A review of treatment modalities for Middle East respiratory syndrome, *J. Antimicrob. Chemother.* 71 (2016) 3340–3350, doi:[10.1093/jac/dkw338](https://doi.org/10.1093/jac/dkw338).
- [62] M.F. Marmor, U. Kellner, T.Y.Y. Lai, R.B. Melles, W.F. Mieler, F. Lum, Recommendations on screening for chloroquine and hydroxychloroquine retinopathy (2016 Revision), *Ophthalmology* 123 (2016) 1386–1394, doi:[10.1016/j.ophtha.2016.01.058](https://doi.org/10.1016/j.ophtha.2016.01.058).
- [63] M.J. Vincent, E. Bergeron, S. Benjannet, B.R. Erickson, P.E. Rollin, T.G. Ksiazek, N.G. Seidah, S.T. Nichol, Chloroquine is a potent inhibitor of SARS coronavirus infection and spread, *Virol. J.* 2 (2005) 1–10, doi:[10.1186/1743-422X-2-69](https://doi.org/10.1186/1743-422X-2-69).
- [64] V.K. Maurya, S. Kumar, A.K. Prasad, M.L.B. Bhatt, S.K. Saxena, Structure-based drug designing for potential antiviral activity of selected natural products from Ayurveda against SARS-CoV-2 spike glycoprotein and its cellular receptor, *Virus Dis.* 31 (2020) 179–193, doi:[10.1007/s13337-020-00598-8](https://doi.org/10.1007/s13337-020-00598-8).
- [65] J. Fantini, C. Di Scala, H. Chahinian, N. Yah, Structural and molecular modelling studies reveal a new mechanism of action of chloroquine and hydroxychloroquine against SARS-CoV-2 infection, *Int. J. Antimicrob. Agents* 55 (2020) 105960, doi:[10.1016/j.ijantimicag.2020.105960](https://doi.org/10.1016/j.ijantimicag.2020.105960).
- [66] M. Hoffmann, H. Kleine-Weber, S. Schroeder, N. Krüger, T. Herrler, S. Erichsen, T.S. Schiergens, G. Herrler, N.H. Wu, A. Nitsche, M.A. Müller, C. Drosten, S. Pöhlmann, SARS-CoV-2 cell entry depends on ACE2 and TMPRSS2 and is blocked by a clinically proven protease inhibitor, *Cell* 181 (2020) 271–280.e8, doi:[10.1016/j.cell.2020.02.052](https://doi.org/10.1016/j.cell.2020.02.052).
- [67] J. Thachil, N. Tang, S. Gando, A. Falanga, M. Cattaneo, M. Levi, C. Clark, T. Iba, ISTH interim guidance on recognition and management of coagulopathy in COVID-19, *J. Thromb. Haemost.* 18 (2020) 1023–1026, doi:[10.1111/jth.14810](https://doi.org/10.1111/jth.14810).
- [68] T. Rathinavel, M. Palanisamy, S. Palanisamy, A. Subramanian, S. Thangaswamy, Phytochemical 6-Gingerol – a promising Drug of choice for COVID-19, *Int. J. Adv. Sci. Eng.* 6 (2020) 1482–1489, doi:[10.29294/ijase.6.4.2020.1482-1489](https://doi.org/10.29294/ijase.6.4.2020.1482-1489).
- [69] H. Noor, A. Ikram, T. Rathinavel, S. Kumarasamy, M. Nasir Iqbal, Z. Bashir, Immunomodulatory and anti-cytokine therapeutic potential of curcumin and its derivatives for treating COVID-19—a computational modeling, *J. Biomol. Struct. Dyn.* (2021) 1–16 0, doi:[10.1080/07391102.2021.1873190](https://doi.org/10.1080/07391102.2021.1873190).
- [70] N. Kumar, A. Awasthi, A. Kumari, D. Sood, P. Jain, T. Singh, N. Sharma, A. Grover, R. Chandra, Antitussive nospapine and antiviral drug conjugates as arsenal against COVID-19: a comprehensive chemoinformatics analysis, *J. Biomol. Struct. Dyn.* (2020) 1–16 0, doi:[10.1080/07391102.2020.1808072](https://doi.org/10.1080/07391102.2020.1808072).
- [71] N. Baildya, N.N. Ghosh, A.P. Chattopadhyay, Inhibitory activity of hydroxychloroquine on COVID-19 main protease: an insight from MD-simulation studies, *J. Mol. Struct.* 1219 (2020) 128595, doi:[10.1016/j.molstruc.2020.128595](https://doi.org/10.1016/j.molstruc.2020.128595).